Narrowband Lumped-Element Microstrip Filters Using Capacitively-Loaded Inductors

Dawei Zhang, *Member, IEEE*, Guo-Chun Liang, *Senior Member, IEEE*, Chien-Fu Shih, Marie E. Johansson, and Richard S. Withers, *Member, IEEE*

***Abstract*— Coupling between microstrip resonators decreases very slowly as a function of the resonator separation. Therefore, it is difficult to realize narrowband filters (e.g. <0.1% fractional bandwidth) in reasonably sized microstrip form due to the very weak coupling values required. In this paper, we report a class of lumped-element filters that uses capacitively-loaded inductors to give frequency-dependent inductance values. A novel frequency-transformation technique is used in the design process. Using this approach, filter bandwidth is determined by the inductance slope of frequency-dependent inductors, $\frac{dL}{d\omega}$. Large coupling capacitance, thus small coupling element separations, can still be used in narrowband microstrip filters to keep the filter layout compact. We present a 5-pole, 0.27% bandwidth $YBa_2Cu_3O_7$ high-temperature superconducting thin film microstrip prototype filter at 900 MHz, which has 1.2 dB insertion loss and 20 dB return loss. It was designed with the coupling capacitors of a 1% bandwidth filter, and then transformed to a 0.27% fractional bandwidth using an appropriate inductance slope parameter, $\frac{dL}{d\omega}$. Measurement showed good agreement with theory.**

I. Introduction

PLANAR FILTERS using high-temperature superconducting thin films have been shown to provide very small insertion loss and superior shape factors [1]–[21]. Unloaded Q-factors of the order of 40,000 have been demonstrated in a microstrip configuration [12]. With such a high Q, microstrip narrowband filters with low insertion loss become possible.

In narrowband microstrip filter designs, the requisite weak coupling is always a challenge. For example, it is hard to realize a very narrowband filter (e.g., <0.1% bandwidth) in the convenient microstrip configuration using conventional coupling schemes due to the slow decay of the coupling as a function of the resonator element separation. To realize the weak coupling required by a narrowband filter, resonator elements in the filter have to be kept very far apart. This requires either a large circuit size or an elaborate package. In those cases, cavity type filters, which are usually quite large in size, or the stripline configuration, which is usually hard to package, often must be used. These approaches will inevitably increase the final system complexity and the engineering cost.

In this paper, a novel approach to solve this weak coupling problem in narrowband filter designs is introduced. Instead of using the conventional coupling approach, frequency-dependent inductors in lumped-element filter circuits are used. Design is accomplished by starting with a wideband conventional filter architecture and applying a frequency transformation to the circuit. This method results in very narrowband filters that other microstrip circuits can not realize, while still using large coupling capacitance in the design to keep the resonator sections close together in a compact form.

Manuscript received March 10, 1995; revised July 10, 1995.
The authors are with Conductus, Inc., Sunnyvale, CA 94086 USA.
IEEE Log Number 9415449.

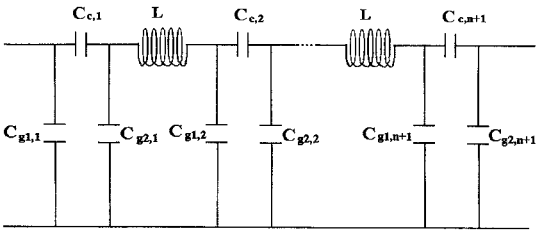

Fig. 1. Topology of the lumped-element filter circuit.

II. Principle of the Frequency Transformation Technique

For simplicity, consider the lumped-element bandpass filter circuit in Fig. 1. In this lumped-element filter circuit, all the inductors are transformed to the same inductance value L. In between adjacent inductors, a π-capacitor network is inserted. Similar π-capacitor networks are also used at the input and output to match the appropriate circuit impedance. For an n-pole bandpass filter, there are n identical inductors and $n+1$ different π-capacitor networks.

In each π-capacitor network, the series capacitor, $C_{c,i}$, is the coupling capacitor between adjacent resonators. Narrowband filters always have very weak coupling between resonators, and require very small values of the coupling capacitors, $C_{c,i}$. In microstrip realizations of this circuit, small $C_{c,i}$ values mean larger resonator separations, that are often difficult to realize due to the limited wafer size.

In this paper, we describe a frequency transformation method to solve this weak coupling problem in the microstrip configuration. Instead of using a pure inductor, we introduce a frequency-dependent inductor, $L(\omega)$, in replacement of the pure inductor. We show that we can realize very narrowband filters without using small coupling capacitance, $C_{c,i}$. The inductor slope parameter, $\frac{dL}{d\omega}$, will control the bandwidth of the filter. Large coupling capacitance, $C_{c,i}$, from the relatively wideband filter circuit prototype, can still be used in narrowband filters.

As is shown in the Appendix (A8), the real filter fractional bandwidth, after using the frequency transformation technique, will be

$$\frac{\Delta\omega}{\omega_0} = \frac{1}{1 + \frac{\omega_0}{2L}\frac{dL'(\omega)}{d\omega}\Big|_{\omega_0}} \frac{\Delta\omega_0}{\omega_0} \tag{1}$$

where ω_0 is the filter center frequency, $\Delta\omega_0$ is the filter bandwidth in the circuit prototype, and $L'(\omega)$ is the frequency-dependent inductance, with $L'(\omega_0) = L$. From this bandwidth transformation relationship, it can be seen that to achieve a narrowband filter, we can actually design a broader bandwidth circuit prototype filter with easily realizable large coupling capacitance, $C_{c,i}$, and then choose an appropriate inductor slope parameter, $\frac{dL}{d\omega}$, to achieve the narrowband filter performance.

It is also shown in the Appendix that after the frequency transformation, the bandwidth of the filter is transformed to either narrower or broader bandwidths, depending on the positive or negative inductor slope parameter, $\frac{dL}{d\omega}$, while the filter response function, S_{21}, is still conserved. This means that a Chebyshev filter design will still conserve the Chebyshev response after bandwidth transformation, a feature that is critical for its applications in various situations of different bandwidths and center frequencies.

III. An Example Circuit Using the Frequency Transformation Technique

To demonstrate the above frequency transformation concept, consider the following example circuit. The specifications of the desired filter are: center frequency $f_0 = 900$ MHz, 5 poles, fractional bandwidth $w = 0.28\%$, passband ripple $L_r = 0.05$ dB.

If Chebyshev response is considered, this filter will require a weakest coupling of -51.1 dB. The coupling capacitance of this -51.1 dB coupling from the circuit prototype in Fig. 1 is too small to reach in microstrip configuration due to poor isolation between resonators in the microstrip configuration. The filter resonator elements would have to be placed very far apart to achieve this weak coupling level. (For an even narrower bandwidth such as 0.05%, the coupling required is only -66.1 dB. It is impossible to build this 0.05% filter using the conventional coupling scheme, especially with the presence of nonadjacent resonator coupling in microstrip configuration.)

If a similar filter is considered with exactly the same specifications, except that the fractional bandwidth is now 1% instead of 0.28%, then this filter will require a weakest coupling of -40 dB. The coupling capacitance of this -40 dB coupling from the circuit prototype in Fig. 1 is easily realizable in microstrip configuration. Starting with this 1% filter design using the topology shown in Fig. 1, followed by the substitution of a frequency dependent inductor $L'(\omega)$ in the designed circuit, we can easily get a new filter which has a bandwidth of 0.28%. The calculated transmission responses of the 1% bandwidth filter and 0.28% bandwidth transformed filter are shown in Fig. 2(a). Also shown, in Fig. 2(b), are the return loss responses of the filter before and after the frequency transformation, with an inductance slope parameter value $\frac{dL'(\omega)}{d\omega}|_{\omega_0} = k = 9.085 \times 10^{-10}$/Hz, and $L'(\omega_0) = 1.752 \times 10^{-8}$ H. From these response curves, we can clearly see that the Chebyshev approximation is still conserved, while the bandwidth of the filter is reduced from 1% to 0.28%, which is the value calculated from the bandwidth transformation equation using the k and L values provided, through the frequency transformation. The realization of this frequency-dependent inductor will be discussed in the next section.

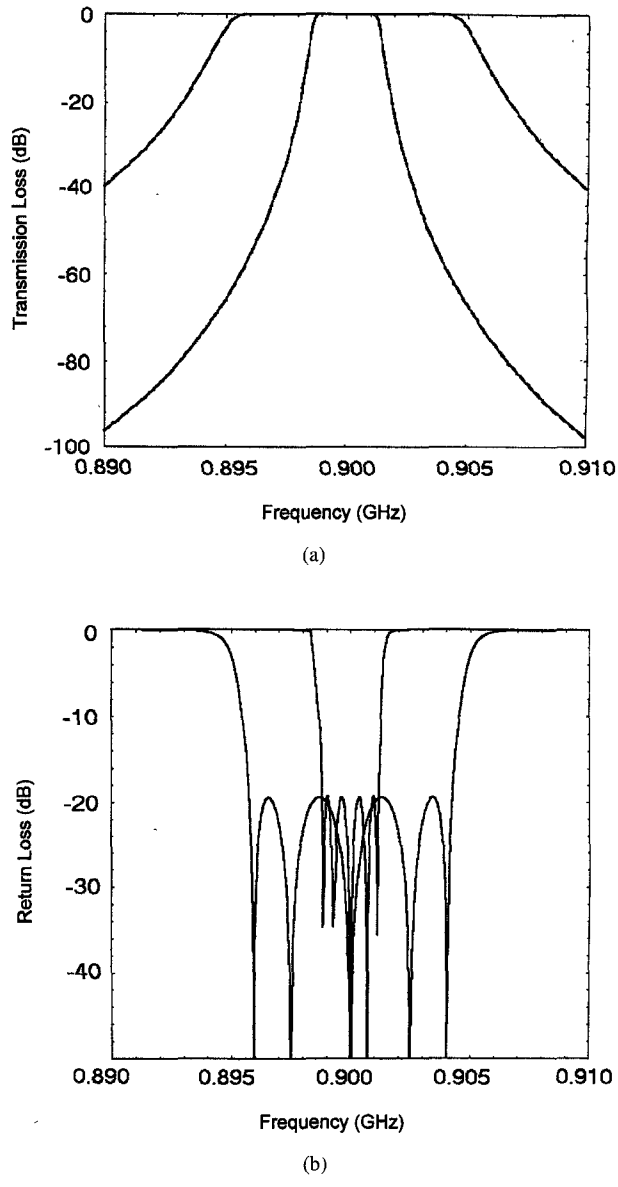

Fig. 2. (a) Calculated transmission loss response from the original 1% bandwidth filter and that of the 0.28% bandwidth filter after frequency transformation. (b) Calculated return loss response from the original 1% bandwidth filter and that of the 0.28% bandwidth filter after frequency transformation.

The deviation of the transmission responses between this 0.28% transformed filter in the ω' domain and that of the original 1% filter in the ω domain (see Appendix for ω and ω' definition) is calculated and plotted in Fig. 3. Within the passband, the maximum deviation from the original Chebyshev function is less than 0.02 dB, while that outside of the passband is less than 0.2 dB at a 40 dB rejection frequency. These numbers show that the Chebyshev function is well preserved even after over a 3-fold reduction in bandwidth.

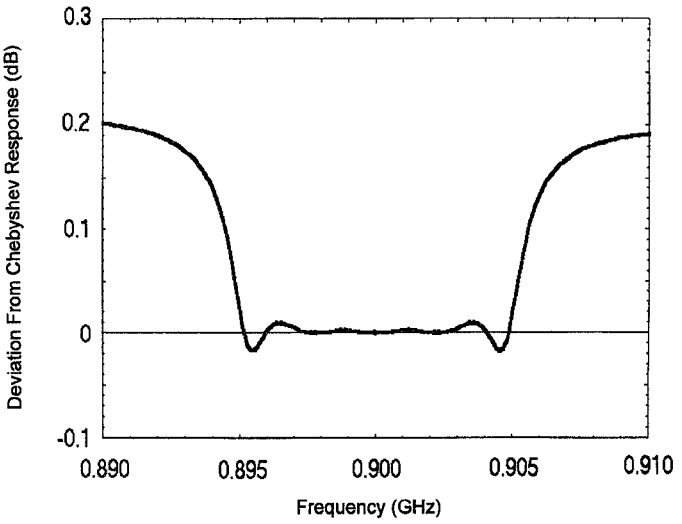

Fig. 3. Deviation in dB from the Chebyshev responses between the 0.28% bandwidth filter in the ω' domain and that of 1% bandwidth filter in the ω domain.

IV. Realization of the Frequency-Dependent Inductors

The key for the frequency transformation technique described above is the slope of the inductance as a function of frequency. In the conventional transmission line realization of inductors, the inductance slope parameter, k, has a negative value because of the parasitic capacitance to ground. Thus, the bandwidth of the lumped-element filters designed using the conventional transmission line approximation of inductors will always have a broader bandwidth than the original circuit prototype. (This phenomenon was reported from measurement in [17].) In order to achieve positive k values, which gives bandwidth transformation to the narrower side, other $L'(\omega)$ mechanisms have to be introduced in the circuit.

One simple realization of $L'(\omega)$ with a positive k is a single capacitor C in parallel with an inductor L_0. From the resultant impedance Z_{eq}

$$\frac{1}{Z_{\text{eq}}} = \frac{1}{j\omega L_0} + j\omega C$$
$$Z_{\text{eq}} = j\omega L'$$

we can calculate the equivalent inductance below $\omega_0 = \frac{1}{\sqrt{L_0 C}}$ as

$$L' = \frac{L_0}{1 - \omega^2 L_0 C} \tag{2}$$

where L_0 is the inductance of the inductor itself and C is the capacitance of the capacitor in parallel with the inductor. The slope parameter

$$k = \left.\frac{dL'(\omega)}{d\omega}\right|_{\omega_0} = \frac{2\omega_0 L_0^2 C}{(1 - \omega_0^2 L_0 C)^2} \tag{3}$$

has a positive value. This parallel L-C component can be easily realized using a half-loop of inductor in parallel with an interdigital capacitor as in Fig. 4.

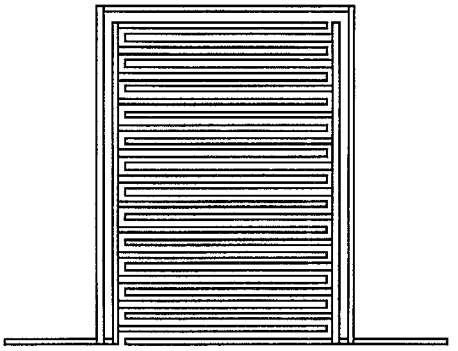

Fig. 4. Layout of a microstrip realization of a frequency-dependent inductor using an interdigital capacitor in parallel with a half-loop inductor.

It should be pointed out that it should be possible to synthesize the filter circuit itself with this parallel L-C in replacement of the original L in Fig. 1. But since this paper is focused on the inductance slope parameter, plus there are many other ways to achieve this frequency-dependent inductance, this L-C circuit synthesis will not be discussed in detail in this paper. It is also understood that the interdigitated capacitor in Fig. 4 has some parasitic series inductance. Since we are considering the total frequency-dependent inductance of this L-C unit, which is modeled by an electromagnetic field simulator, those parasitic effects should have been considered already.

V. Measurement on a 0.3% Bandwidth Prototype Filter

In this section, we demonstrate the validity of the frequency transformation technique by experimentally constructing a narrowband filter. To demonstrate the concept, we first report a 2-pole, 0.3% bandwidth bandpass filter at 900 MHz in microstrip form using superconducting niobium, and then show a measured response of a 5-pole, 0.27% bandwidth filter at 900 MHz using $YBa_2Cu_3O_7$ high-temperature superconducting thin film.

The prototype filter is built as follows: First, a relatively broadband filter circuit prototype (realizable coupling capacitors) is chosen with 1% bandwidth. The inductor and capacitor values are obtained for this 1% bandwidth filter. Second, for the desired bandwidth of 0.3%, the inductor slope parameter required is calculated from the bandwidth transformation equation

$$\frac{\Delta\omega}{\omega_0} = \frac{1}{1 + \frac{\omega_0}{2L}\frac{dL'(\omega)}{d\omega}|_{\omega_0}} \frac{\Delta\omega_0}{\omega_0}.$$

Third, the inductance slope parameter is realized from the equation $L' = \frac{L_0}{1-\omega^2 L_0 C}$ using the approach in the above section, and the parallel capacitance is obtained. Fourth, by realizing all the individual values of the inductors and capacitors, we will have a 0.3% bandwidth filter, while still using the more easily achievable large coupling capacitance from the 1% bandwidth filter circuit prototype. Fig. 5 shows the layout of a 2-pole 0.3% bandwidth filter, and Fig. 6 shows the measured 0.3% bandwidth filter response, as well as the

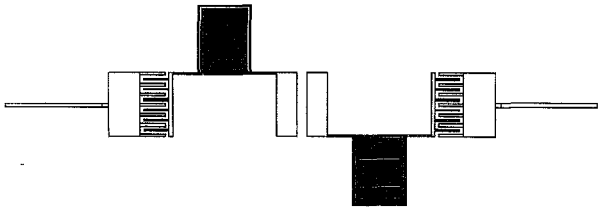

Fig. 5. Layout of a 2-pole, 0.3% bandwidth filter realized on microstrip using the frequency transformation technique.

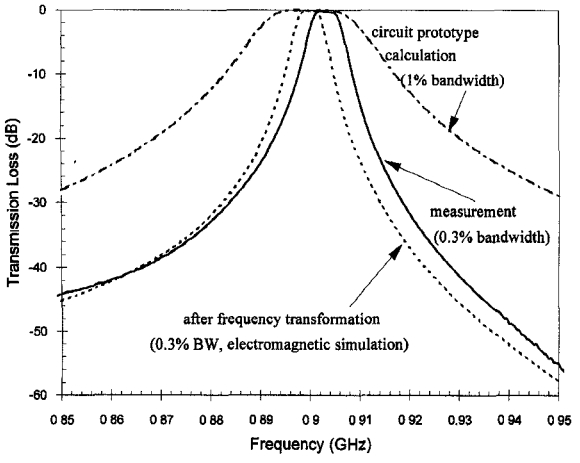

Fig. 6. Measured transmission response of the 2-pole 0.3% bandwidth filter using a Nb superconducting microstrip structure, as well as that calculated for the 1% bandwidth filter circuit prototype and a full-wave electromagnetic simulation result.

1% bandwidth circuit prototype response and the 0.3% bandwidth simulation response from a full-wave electromagnetic simulator. This clearly demonstrates that the filter bandwidth is truly transformed from the 1% circuit prototype to the 0.3% desired bandwidth.

To show the usefulness of this frequency transformation technique in real filter applications, we built a 5-pole bandpass filter at 900 MHz with 0.27% bandwidth using double-sided $YBa_2Cu_3O_7$ high-temperature superconducting thin films on $LaALO_3$ substrate, operating at 77 K. The layout of the filter is shown in Fig. 7. The measured response of this 5-pole 0.27% filter is shown in Fig. 8. This filter was also designed with coupling of a 1% bandwidth filter and then transformed to 0.27% bandwidth using an appropriate inductance slope parameter. Due to the dielectric constant variations across the $LaAlO_3$ substrate (twinning effect), this filter response was obtained with tuning.

VI. Conclusion

In conclusion, we have developed a new class of lumped-element filters that uses capacitively-loaded inductors to form frequency-dependent inductor values. A novel frequency transformation technique is applied to transform the filter bandwidth from the wideband circuit prototypes to narrowband filters. Using this technique, equivalent weak couplings, and therefore very narrowband filters, can be realized in a microstrip configuration. This frequency transformation method

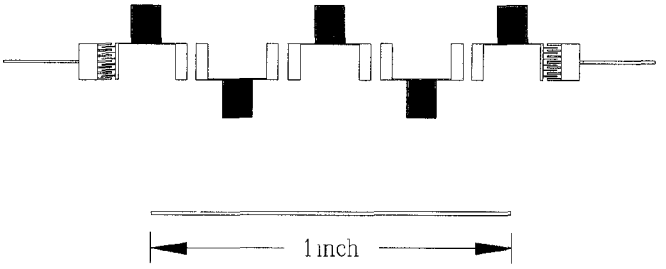

Fig. 7. Layout of a 5-pole, 0.27% bandwidth filter realized on microstrip using the frequency transformation technique.

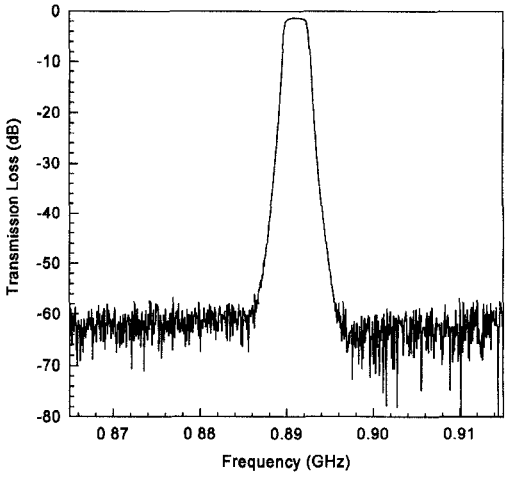

(a)

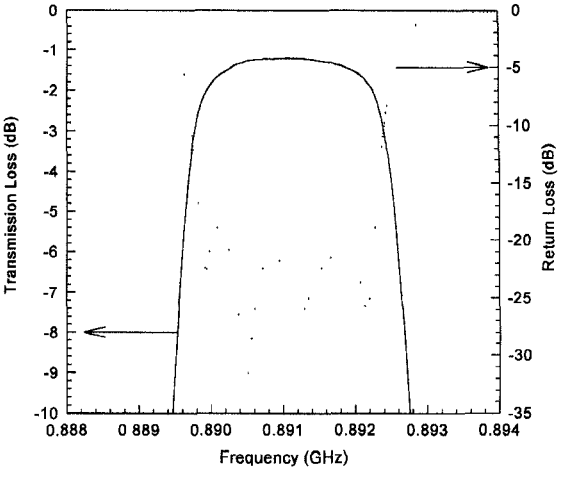

(b)

Fig. 8. (a) Measured transmission response of the 5-pole, 0.27% bandwidth filter using $YBa_2Cu_3O_7$ high-temperature superconducting thin film microstrip at 77 K. (b) An expanded view of the measured transmission loss and return loss response of the 5-pole, 0.27% bandwidth filter using $YBa_2Cu_3O_7$ high-temperature superconducting thin film microstrip at 77 K.

was also verified in a 5-pole 0.27% bandwidth prototype filter design at 900 MHz fabricated using a $YBa_2Cu_3O_7$ high-temperature superconducting thin film microstrip configuration. Measurement showed a 1.2 dB insertion loss and a 20 dB return loss.

APPENDIX

The total transmission response of the circuit, S_{21}, can be calculated from the multiplication of the ABCD-matrix of each individual element followed by the transformation of the total ABCD-matrix to the scattering S-matrix.

Assuming the ABCD-matrix of each inductor element is A_L, and those of the π-capacitor networks are $A_{\pi i}$, as shown in Fig. 1, where $i = 1, 2, 3, \ldots, n+1$, then we have

$$A_L = \begin{pmatrix} 1 & j\omega L \\ 0 & 1 \end{pmatrix} \tag{A1}$$

$$A_{\pi i} = \begin{pmatrix} 1 & 0 \\ j\omega C_{g1,i} & 1 \end{pmatrix} \begin{pmatrix} 1 & \frac{1}{j\omega C_{c,i}} \\ 0 & 1 \end{pmatrix} \begin{pmatrix} 1 & 0 \\ j\omega C_{g2,i} & 1 \end{pmatrix} = \begin{pmatrix} 1 + \frac{C_{g2,i}}{C_{c,i}} & \frac{1}{j\omega C_{c,i}} \\ j\omega \frac{(C_{c,i}C_{g1,i} + C_{c,i}C_{g2,i} + C_{g1,i}C_{g2,i})}{C_{c,i}} & 1 + \frac{C_{g1,i}}{C_{c,i}} \end{pmatrix} \tag{A2}$$

where i is the ith number of the π-capacitor networks, $i = 1, 2, 3, \ldots, n+1$, $C_{c,i}$ is the coupling capacitor, $C_{g1,i}$ and $C_{g2,i}$ are the grounding capacitors for the same ith π-capacitor network.

The total ABCD-matrix of the filter circuit is then

$$A = A_{\pi 1} A_L A_{\pi 2} \ldots A_{\pi i} A_L A_{\pi,i+1} \ldots A_{\pi,n} A_L A_{\pi,n+1} = \begin{pmatrix} a & b \\ c & d \end{pmatrix}. \tag{A3}$$

It is clear that the ABCD-matrix of a one-pole filter is

$$A_1 = A_{\pi 1} A_L A_{\pi 2} = \begin{pmatrix} a_1 & \frac{jb_1}{\omega} \\ j\omega c_1 & d_1 \end{pmatrix} \tag{A3a}$$

$$a_1 = \left(1 + \frac{C_{g2,1}}{C_{c,1}}\right) + \left(1 + \frac{C_{g2,2}}{C_{c,2}}\right) + \frac{(C_{g1,2}C_{c,2} + C_{g1,2}C_{g2,2} + C_{c,2}C_{g2,2})}{C_{c,1}C_{c,2}} \times [1 - (C_{c,1} + C_{g2,1})L\omega^2]$$

$$b_1 = \frac{\left(1 + \frac{C_{g1,2}}{C_{c,2}}\right)[-1 + (C_{c,1} + C_{g2,1})L\omega^2]}{C_{c,1}} - \frac{\left(1 + \frac{C_{g2,1}}{C_{c,1}}\right)}{C_{c,2}}$$

$$c_1 = \frac{(C_{g1,1}C_{c,1} + C_{g1,1}C_{g2,1} + C_{c,1}C_{g2,1})\left(1 + \frac{C_{g2,2}}{C_{c,2}}\right)}{C_{c,1}} + \frac{(C_{g1,2}C_{c,2} + C_{g1,2}C_{g2,2} + C_{c,2}C_{g2,2})}{C_{c,2}} \times \left[1 + \frac{C_{g1,1}}{C_{c,1}} - \frac{(C_{g1,1}C_{c,1} + C_{g1,1}C_{g2,1} + C_{c,1}C_{g2,1})}{C_{c,1}} L\omega^2\right]$$

$$d_1 = \frac{(C_{g1,1}C_{c,1} + C_{g1,1}C_{g2,1} + C_{c,1}C_{g2,1})}{C_{c,1}C_{c,2}} + \left(1 + \frac{C_{g1,2}}{C_{c,2}}\right) \times \left[1 + \frac{C_{g1,1}}{C_{c,1}} - \frac{(C_{g1,1}C_{c,1} + C_{g1,1}C_{g2,1} + C_{c,1}C_{g2,1})}{C_{c,1}} L\omega^2\right].$$

The ABCD-matrix of a two-pole filter is $A_2 = A_1 A_L A_{\pi,3} = A_1 A_{LC}$, which is the product of the one-pole ABCD-matrix and the ABCD-matrix of an inductor and a π-capacitors, A_{LC}. The latter can be expressed as

$$A_{LC} = A_L A_{\pi 3} = \begin{pmatrix} a_{LC} & \frac{jb_{LC}}{\omega} \\ j\omega c_{LC} & d_{LC} \end{pmatrix} \tag{A3b}$$

$$a_{LC} = 1 + \frac{C_{g2,3}}{C_{c,3}} - \frac{(C_{g1,3}C_{c,3} + C_{g1,3}C_{g2,3} + C_{c,3}C_{g2,3})L\omega^2}{C_{c,3}}$$

$$b_{LC} = \frac{[-1 + (C_{g1,3} + C_{c,3})L\omega^2]}{C_{c,3}}$$

$$c_{LC} = \frac{(C_{g1,3}C_{c,3} + C_{g1,3}C_{g2,3} + C_{c,3}C_{g2,3})}{C_{c,3}}$$

$$d_{LC} = 1 + \frac{C_{g1,3}}{C_{c,3}}.$$

Noting that a_1, b_1, c_1, d_1, and $a_{LC}, b_{LC}, c_{LC}, d_{LC}$ are only functions of $L\omega^2$, we can conclude that the final two-pole ABCD-matrix, A_2, will also has the form of (A3a). Further more, any i-pole filter ABCD-matrix can be expressed as the product of that of the $(i-1)$-pole and that of an inductor and a π-capacitors, A_{LC}. Cascading all the argument above, we can show that the matrix elements, a, b, c, d, of the total ABCD-matrix in (A3), will have the following symmetry

$$\begin{aligned} a &= a_0 + a_1(L\omega^2) + a_2(L\omega^2)^2 + \cdots + a_n(L\omega^2)^n \\ b &= \frac{1}{j\omega}[b_0 + b_1(L\omega^2) + b_2(L\omega^2)^2 + \cdots + b_n(L\omega^2)^n] \\ c &= j\omega[c_0 + c_1(L\omega^2) + c_2(L\omega^2)^2 + \cdots + c_n(L\omega^2)^n] \\ d &= d_0 + d_1(L\omega^2) + d_2(L\omega^2)^2 + \cdots + d_n(L\omega^2)^n. \end{aligned} \tag{A4}$$

Here all coefficients, a_i, b_i, c_i, d_i, $i = 0, 1, 2, 3, \ldots, n$, are real numbers and functions of capacitance only, while $L\omega^2$ are always linked together as a variable.

The S-matrix can be calculated from the above ABCD-matrix. Assuming the input and output impedance is Z_1 and Z_2, the transmission response of the filter, S_{21}, is then

$$S_{21} = \frac{2\sqrt{Z_1 Z_2}}{Z_2 a + b + Z_1 Z_2 c + Z_1 d} \tag{A5}$$

where a and d are pure real numbers, while b and c are pure imaginary.

From (A4) and (A5), we can see that if a frequency transformation can be introduced, which keeps $L\omega^2$ invariant, then a and d, which contribute to the real part of the denominator in S_{21}, will keep unchanged. Further more, if changes caused by the frequency transformation due to the $j\omega$ part in b and c are small enough (which is exactly equal to zero at the filter passband center, ω_0), then the imaginary part of the denominator in S_{21} will keep invariant too. So finally, the whole transmission response S_{21} will keep unchanged after the frequency transformation. The invariance of the imaginary part of the denominator in S_{21} will be discussed in the later part of this section.

The purpose of the frequency transformation is basically to introduce a frequency dependent inductance $L'(\omega)$ to replace the original inductance L. $L'(\omega)$ is chosen to have the same value as L at the filter passband center, $L'(\omega_0) = L$. The invariance of the S_{21} to the transformation will simply couple the slope of L to the scaling of the frequency ω. So finally the bandwidth of the filter will either shrink due to the positive slope in $L'(\omega)$, or expand due to the negative slope in $L'(\omega)$. This kind of bandwidth transformation is very useful especially for ultra-narrow-band filters (e.g. 0.05%) for superconductor applications, where the circuit Q of the superconducting microstrip circuit is over 40,000 while the difficulties in achieving weak (e.g., −60 dB) coupling capacitance prevents the realization of the ultra-narrow-band filters.

To conduct such a transformation, we define another frequency domain, ω', so that

$$L'(\omega)\omega^2 = L\omega'^2 \tag{A6}$$

or

$$\omega' = \sqrt{\frac{L'(\omega)}{L}}\omega. \tag{A7}$$

According to the argument above, the transformation equation (A7) will guarantee the invariance of the filter response function, S_{21}, in ω' scale, compared to the original response function in ω scale before the transformation.

To calculate the filter real bandwidth after transformation, we take the derivative of (A7), which yields

$$d\omega' = d\left(\sqrt{\frac{L'(\omega)}{L}}\omega\right) = \sqrt{\frac{L'(\omega)}{L}}d\omega + \omega d\left(\sqrt{\frac{L'(\omega)}{L}}\right)$$
$$= \left[\sqrt{\frac{L'(\omega)}{L}} + \frac{\omega}{2L}\sqrt{\frac{L}{L'(\omega)}}\frac{dL'(\omega)}{d\omega}\right]d\omega.$$

Using $L'(\omega_0) = L$, we have the bandwidth relationship as

$$\Delta\omega' = \left[1 + \frac{\omega_0}{2L}\frac{dL'(\omega)}{d\omega}\bigg|_{\omega_0}\right]\Delta\omega$$

where $\Delta\omega'$ is the bandwidth in ω' domain, which is also the original filter bandwidth, $\Delta\omega_0$, before the transformation due to the invariance of the response function, while $\Delta\omega$ is the new real bandwidth after the transformation. Thus we can calculate the new bandwidth after the transformation as

$$\frac{\Delta\omega}{\omega_0} = \frac{1}{1 + \frac{\omega_0}{2L}\frac{dL'(\omega)}{d\omega}\big|_{\omega_0}}\frac{\Delta\omega_0}{\omega_0}. \tag{A8}$$

Equation (A8) shows that the filter bandwidth is transformed by a factor of $\left[1 + \frac{\omega_0}{L}\frac{dL'(\omega)}{d\omega}|_{\omega_0}\right]^{-1}$.

To prove that the change in $j\omega$ term in b and c due to the frequency transformation is small enough to be neglected, we define

$$B = [b_0 + b_1(L\omega^2) + b_2(L\omega^2)^2 + \cdots + b_n(L\omega^2)^n]$$
$$C = [c_0 + c_1(L\omega^2) + c_2(L\omega^2)^2 + \cdots + c_n(L\omega^2)^n]. \tag{A9}$$

So we have

$$b = \frac{1}{j\omega}B(\omega) = \sqrt{\frac{L'(\omega)}{L}}\frac{1}{j\omega'}B(\omega')$$
$$c = j\omega C(\omega) = \sqrt{\frac{L}{L'(\omega)}}j\omega' C(\omega'). \tag{A10}$$

In narrow-band approximation, $L'(\omega)$ takes the form $L'(\omega) = L[1 + k(\omega - \omega_0)]$, where k is the slope coefficient which is very small, $|k(\omega - \omega_0)| \ll 1$. Thus we have

$$b \approx \left[1 + \frac{k}{2}(\omega - \omega_0)\right]\frac{1}{j\omega'}B(\omega')$$
$$c \approx \left[1 - \frac{k}{2}(\omega - \omega_0)\right]j\omega' C(\omega'). \tag{A11}$$

Then the imaginary part in the denominator of equation (A5) is

$$b(\omega) + Z_1Z_2c(\omega) = \left[1 + \frac{k}{2}(\omega - \omega_0)\right]\frac{1}{j\omega'}B(\omega')$$
$$+ Z_1Z_2\left[1 - \frac{k}{2}(\omega - \omega_0)\right]j\omega' C(\omega')$$
$$= \frac{1}{j\omega'}B(\omega') + Z_1Z_2j\omega' C(\omega')$$
$$+ \frac{k}{2}(\omega - \omega_0)$$
$$\times \left[\frac{1}{j\omega'}B(\omega') - Z_1Zj\omega' C(\omega')\right]$$
$$= b(\omega') + Z_1Z_2c(\omega') + \frac{k}{2}(\omega - \omega_0)$$
$$\times \left[\frac{1}{j\omega'}B(\omega') - Z_1Zj\omega' C(\omega')\right]$$
$$\approx b(\omega') + Z_1Z_2c(\omega').$$

ACKNOWLEDGMENT

The authors would like to thank A. Dela Cruz for niobium superconducting circuit processing, R. C. Yu for computer data acquisition, and T. Luong and Q. Thai for filter tuning.

REFERENCES

[1] G. L. Matthaei and G. L. Hey-Shipton, "Novel staggered resonator array superconducting 2.3 GHz bandpass filters," in *1993 IEEE Microwave Symp. Dig.*, Atlanta, Georgia, June 1993, pp. 1269–1272.

[2] ——, "High-temperature superconducting 8.45-GHz bandpass filter for the deep space network," in *1993 IEEE Microwave Symp. Dig.*, Atlanta, Georgia, June 1993, pp. 1273–1276.

[3] W. G. Lyons, R. S. Withers, J. M. Hamm, A. C. Anderson, P. M. Mankiewich, M. L. O'Malley, R. E. Howard, R. R. Bonetti, A. E. Williams, and N. Newman, "High-temperature superconductive passive microwave devices," in *1991 IEEE Int. Microwave Symp. Dig.*, Boston, MA, June 1991, pp. 1227–1230.

[4] S. H. Talisa, M. A. Janocko, C. Moskowitz, J. Talvacchio, J. F. Billing, R. Brown, D. C. Buck, C. K. Jones, B. R. McAvoy, G. R. Wagner, and D. H. Watt, "Low- and high-temperature superconducting microwave filters," *IEEE Trans. Microwave Theory Tech.*, vol. 39, pp. 1448–1454, Sept. 1991.

[5] R. R. Mansour, "Design of superconductive multiplexers using single-mode and dual-mode filters," *IEEE Trans. Microwave Theory Tech.*, vol. 42, no. 7, pp. 1411–1418, July 1994.

[6] R. R. Bonetti and A. E. Williams, "Preliminary design steps for thin-film superconductor filters," in *1990 IEEE Int. Microwave Symp. Dig.*, Dallas, TX, May 1990, pp. 273–276.

[7] J. A. Curtis and S. J. Fiedziuszko, "Miniature dual mode microstrip filters," in *1991 IEEE Int. Microwave Symp. Dig.*, Boston, MA, June 1991, pp. 443–446.
[8] A. Fathy, D. Kalokitis, V. Pendrick, E. Belohoubek, A. Pique, and M. Mathur, "Superconducting narrow band pass filters for advanced multiplexers," in *1993 IEEE Int. Microwave Symp. Dig.*, Atlanta, GA, June 1993, pp. 1277–1280.
[9] H. S. Newman, D. B. Chrisey, and J. S. Horwitz, "Microwave devices using $YBa_2Cu_3O_{7-\delta}$ films made by pulsed laser deposition," *IEEE Trans. Magn.*, vol. 27, no. 2, pp. 2540–2543, Mar. 1991.
[10] S. J. Hedges and R. G. Humphreys, "Extracted pole planar elliptic function filters," in *Proc. ESA/ESTEC Workshop on Space Applications of High-Temperature Superconductors*, Noordwijk, Apr. 1993, pp. 97–106.
[11] M. S. Schmidt, R. J. Forse, R. B. Hammond, M. M. Eddy, and W. L. Olson, "Measured performance at 77 K of superconducting microstrip resonators and filters," *IEEE Trans. Microwave Theory Tech.*, vol. 39, pp. 1475–1479, Sept. 1991.
[12] D. Zhang, G.-C. Liang, C. F. Shih, R. S. Withers, M. E. Johansson, and A. Dela Cruz, "Compact forward-coupled superconducting microstrip filters for cellular communication," *1994 Applied Superconductivity Conf.*, Boston, MA, Oct. 1994.
[13] D. Zhang, G.-C. Liang, C. F. Shih, M. E. Johansson, and R. S. Withers, "Accurate design of compact forward-coupled microstrip filters using an integral-equation field solver," to be published in *Int. J. Microwave and Millimeter-Wave Computer-Aided Eng.*, vol. 5, no. 5, 1995.
[14] D. Zhang, G.-C. Liang, C. F. Shih, and R. S. Withers, "Narrowband lumped-element microstrip filters using capacitively-loaded inductors," in *1995 IEEE Int. Microwave Symp. Dig.*, Orlando, FL, May 1995, pp. 379–382.
[15] D. Zhang, G.-C. Liang, C. F. Shih, Z. H. Lu, and M. E. Johansson, "A 19-pole cellular bandpass filter using 75-mm-diameter high-temperature superconducting thin films," to be published in *IEEE Trans. Microwave and Guided Wave Lett.*.
[16] D. G. Swanson, "Thin-film lumped-element microwave filters," in *1989 IEEE Int. Microwave Symp. Dig.*, Long Beach, CA, June 1989, pp. 671–674.
[17] D. G. Swanson Jr, R. Forse, and B. J. L. Nilsson, "A 10 GHz thin film lumped-element high temperature superconducting filter," in *1992 IEEE Int. Microwave Symp. Dig.*, Albuquerque, NM, June 1992, pp. 1191–1193.
[18] S. Ye and R. R. Mansour, "Design of manifold-coupled multiplexers using superconducting lumped-element filters," in *1994 IEEE Int. Microwave Symp. Dig.*, San Diego, CA, May 1994, pp. 191–194.
[19] G.-C. Liang, D. Zhang, C. F. Shih, R. S. Withers, M. E. Johansson, W. Ruby. B. F. Cole, M. Krivoruchko, and D. E. Oates, "High power HTS microstrip filters for wireless communication," in *1994 IEEE Int. Microwave Symp. Dig.*, San Diego, CA, May 1994, pp. 183–186.
[20] G.-C. Liang, D. Zhang, C. F. Shih, M. E. Johansson, R. S. Withers, D. E. Oates, and A. C. Anderson, "High power HTS microstrip filters for cellular base-station application," *1994 Applied Superconductivity Conf.*, Boston, MA, Oct. 1994.
[21] G.-C. Liang, D. Zhang, C. F. Shih, M. E. Johansson, R. S. Withers, A. C. Anderson, D. E. Oates, P. Polakos, P Mankiewich, E. de Obaldia, and R. E. Miller, "High-temperature superconducting microstrip filters with high power-handling capability," in *1995 IEEE Int. Microwave Symp. Dig.*, Orlando, FL, May 1995, pp. 191–194.

Dawei Zhang (M'93), for a photograph and biography, see this issue p. 3028.

Guo-Chun Liang, (S'87-M'90–SM'94) for a photograph and biography, see this issue p. 3028.

Chien-Fu Shih, for a photograph and biography, see this issue p. 3028.

Marie E. Johansson, for a photograph and biography, see this issue p. 3028.

Richard S. Withers, (M'78) for a photograph and biography, see this issue p. 3029.